Synthesis and Characterization of a Binuclear Palladium(I) Complex with Bridging η^3-Indenyl Ligands, $Pd_2(\mu\text{-}\eta^3\text{-indenyl})_2(\text{isocyanide})_2$, and Its Transformation to a Tetranuclear Palladium(I) Cluster of Isocyanides, $Pd_4(\mu\text{-acetate})_4(\mu\text{-isocyanide})_4$†

Tomoaki Tanase, Takahito Nomura, Toshihiro Fukushima, and Yasuhiro Yamamoto*

Department of Chemistry, Faculty of Science, Toho University, Miyama, Funabashi, Chiba 274, Japan

Kimiko Kobayashi

RIKEN (Institute of Physical and Chemical Research), Wako, Saitama 351, Japan

Received March 25, 1993®

The reaction of $PdCl_2(RNC)_2$ (RNC = isocyanide) with lithium indenyl (LiIn) gave binuclear palladium(I) complexes, $Pd_2(\mu\text{-}\eta^3\text{-In})_2(RNC)_2$ (**3a**, R = ^{t}Bu; **3b**, R = 2,6-$Me_2C_6H_3$; **3c**, R = 2,4,6-$Me_3C_6H_2$; **3d**, R = 2,4,6-$^t Bu_3C_6H_2$) in moderate yields. Complex **3** was characterized by elemental analysis, IR, UV–vis, and ^{1}H and ^{13}C NMR spectroscopies, and X-ray crystallography. Compound **3a** crystallizes in the monoclinic system, space group $P2_1/n$, with a = 17.254(8) Å, b = 9.442(6) Å, c = 17.252(6) Å, β = 113.11(3)°, and Z = 4 (R = 0.061 and R_w = 0.049 for 1930 independent reflections with $I > 2.5\sigma(I)$), and compound **3b** crystallizes in the monoclinic system, space group $P2_1/n$, with a = 19.235(3) Å, b = 9.857(6) Å, c = 15.989(9) Å, β = 97.32(3)°, and Z = 4 (R = 0.059 and R_w = 0.070 for 3250 reflections with $I > 2.5\sigma(I)$). Complex **3** consists of two palladium atoms bridged by two η^3-indenyl groups in a *syn* arrangement. The Pd–Pd bond lengths are 2.644(3) Å (**3a**) and 2.656(2) Å (**3b**). The two indenyl groups are in a wedge-shaped arrangement, with the dihedral angles of 66.5° (**3a**) and 47.7° (**3b**) between the two indenyl planes. The array of $Pd_2(RNC)_2$ unit is an A-frame form; the average Pd–Pd–C_{RNC} angles are 153.0° (**3a**) and 163.7° (**3b**). Complex **3** treated with acetic acid is readily transformed to a tetranuclear palladium(I) cluster of isocyanides, $Pd_4(\mu\text{-OAc})_4(\mu\text{-RNC})_4$ (**5a**, R = ^{t}Bu; **5b**, R = 2,6-$Me_2C_6H_3$). Cluster **5a** crystallizes in the monoclinic system, space group $C2/m$ with a = 18.782(9) Å, b = 18.034(9) Å, c = 13.420(9) Å, β = 100.07(4)°, and Z = 4 (R = 0.061 and R_w = 0.064 for 2413 reflections with $I > 3\sigma(I)$). The four palladium atoms lie in a rectangular array with the short Pd–Pd bonds (average 2.650 Å) bridged by isocyanides and the long Pd–Pd bonds (average 2.894 Å) bridged by acetate ligands. The bridging isocyanides are almost linear (average C–N–C angle = 172°). Extended Hückel MO calculations of the model compounds $[Pd_4(\mu\text{-}O_2CH)_4(\mu\text{-HNC})_4]$ (**8**) and $[Pd_2(\mu\text{-HNC})_2(OH)_4]_2^{4-}$ (**9**) were carried out to elucidate the metal–metal bonding systems.

Introduction

The η^5-indenyl transition metal complexes are known to be more reactive for associative reactions than their cyclopentadienyl analogues, because the reversible slippage of the metal across the five-membered ring can form a reactive η^3-indenyl tautomer that has both benzenoid resonance stabilization and an accessible coordination site (so-called "indenyl effect")[1,2] In this regard, η^3-indenyl complexes postulated as intermediates have attracted much attention, but the structural studies of such complexes are still rare and are limited to the monomeric species, e.g. $W(\eta^5\text{-In})(\eta^3\text{-In})(CO)_2$,[3] $V(\eta^5\text{-In})(\eta^3\text{-In})(CO)_2$,[4] $Ir(\eta^3\text{-In})(PMe_2Ph)_3$,[5] and $[Fe(\eta^3\text{-In})(CO)_3]^-$.[6] Werner et al. have reported the structural study of the binuclear palladium complex $Pd_2(\mu\text{-}\eta^3\text{-Cp})_2(PR_3)_2$ (**1**) (Cp = cyclopentadienyl), in which two η^3-Cp ligands are coordinated sandwichlike to the linear $Pd_2(PR_3)_2$ unit in an *anti* arrangement.[7] One of the Cp ligands of **1** was easily displaced by acetate and thiolate anions without cleavage of the metal–metal bond to give $Pd(\mu\text{-}\eta^3\text{-Cp})(\mu\text{-X})(PR_3)_2$ (**2a**, X = CH_3COO^-; **2b**, X = RS^-).[8] Further, the reaction of **2a** with $Na[M(\eta\text{-Cp})(CO)_3]$ (M = Cr, Mo) afforded the heteronuclear Pd_2M cluster $Pd_2M(\eta^5\text{-Cp})(\mu\text{-}\eta^3\text{-Cp})(\mu_2\text{-CO})_2)(\mu_3\text{-CO})(PR_3)_2$.[8] These reactions provided a new route into the field of mixed-metal clusters.[9] In contrast with Cp complexes, dimeric complexes with bridging η^3-indenyl groups have not been prepared thus far.

We have studied the synthesis and characterization of binuclear, trinuclear and high nuclear platinum and palladium complexes containing isocyanide ligands.[10–16] Recently, bidentate diphosphines were introduced as supporting ligands for the M–M bond, and it was revealed that the length of methylene chain of

† Studies on Interactions of Isocyanide with Transition Metal Complexes. 36. For part 35, see: Yamamoto, Y.; Tanase, T.; Yanai, T.; Asano, T.; Kobayashi, K. *J. Organomet. Chem.*, in press.

® Abstract published in *Advance ACS Abstracts*, September 15, 1993.

(1) Habib, A.; Tanke, R. S.; Holt, E. M.; Crabtree, R. H. *Organometallics* **1989**, *8*, 1225.
(2) O'Connor, J. M.; Casey, C. P. *Chem. Rev.* **1987**, *87*, 307.
(3) Nesmeyanov, A. N.; Ustynyuk, N. A.; Makarova, L. G.; Andrianov, V. G.; Struchkov, Yu. T.; Andrae, S.; Ustynyuk, Yu. A.; Malyugina, S. G. *J. Organomet. Chem.* **1978**, *159*, 189.
(4) Kowaleski, R. M.; Rheingold, A. L.; Trogler, W. C.; Basolo, F. *J. Am. Chem. Soc.* **1986**, *108*, 2461.
(5) Merola, J. S.; Kacmarcik, R. T.; Engen, D. V. *J. Am. Chem. Soc.* **1986**, *108*, 329.
(6) Forschner, T. C.; Cutler, A. R.; Kullnig, R. K. *Organometallics*, **1987**, *6*, 889.
(7) Werner, H.; Kraus, H. J.; Schubert, U.; Ackermann, K. *Chem. Ber.* **1982**, *115*, 2905.
(8) Werner, H.; Kraus, H. J.; Thometzek, P. *Chem. Ber.* **1982**, *115*, 2914.
(9) Thometzek, P.; Werner, H. *Organometallics* **1987**, *6*, 1169.
(10) Yamamoto, Y.; Yamazaki, H. *Bull. Chem. Soc. Jpn.* **1985**, *58*, 1843.
(11) Yamamoto, Y.; Yamazaki, H. *Inorg. Chem.* **1986**, *25*, 3327.
(12) Yamamoto, Y.; Yamazaki, H. *J. Chem. Soc., Dalton Trans.* **1986**, 677.
(13) (a) Yamamoto, Y.; Takahashi, K.; Yamazaki, H. *Chem. Lett.* **1985**, 201. (b) Yamamoto, Y.; Takahashi, K.; Matsuda, K.; Yamazaki, H. *J. Chem. Soc., Dalton Dalton.* **1987**, 1833.
(14) (a) Yamamoto, Y.; Aoki, K.; Yamazaki, H. *Chem. Lett.* **1979**, 391. (b) Yamamoto, Y.; Aoki, K.; Yamazaki, H. *Organometallics* **1983**, *2*, 1377.
(15) (a) Yamamoto, Y.; Yamazaki, H.; Sakurai, T. *J. Am. Chem. Soc.* **1982**, *104*, 2329. (b) Yamamoto, Y.; Yamazaki, H. *J. Chem. Soc., Dalton Trans.* **1989**, 2161.
(16) (a) Yamamoto, Y.; Takahashi, K.; Yamazaki, H. *J. Am. Chem. Soc.* **1986**, *108*, 2458. (b) Yamamoto, Y.; Yamazaki, H. *Organometallics* **1993**, *12*, 933.

0020-1669/93/1332-4578$04.00/0

Table I. Crystallographic and Experimental Data for **3a**, **3b**, and **5a**

	3a	3b	5a
formula	$C_{28}H_{32}N_2Pd_2$	$C_{36}H_{32}N_2Pd_2$	$C_{28}N_{48}N_4Pd_4O_8 \cdot C_6H_6$
fw	609.37	705.51	1072.42
cryst syst	monoclinic	monoclinic	monoclinic
space group	$P2_1/n$ (No. 14)	$P2_1/n$ (No. 14)	$C2/m$ (No. 12)
lattice const, Å and deg	a = 17.254(8)	a = 19.235(3)	a = 18.782(9)
	b = 9.442(6)	b = 9.857(6)	b = 18.034(9)
	c = 17.252(6)	c = 15.989(9)	c = 13.420(9)
	β = 113.11(3)	β = 97.32(3)	β = 100.07(4)
V, Å^3	2585	3006	4475
Z	4	4	4
T, °C	23	23	23
D_{calcd}, g cm^{-3}	1.566	1.559	1.592
μ, min^{-1}	1.39	1.21	1.61
no. of unique data	1930 ($I > 2.5\sigma(I)$)	3250 ($I > 2.5\sigma(I)$)	2413 ($I > 3\sigma(I)$)
no. of params	289	361	184
R^a	0.061	0.059	0.061
R_w	0.049	0.070	0.064

^{a} $R = \sum\|F_o| - |F_c\|/\sum|F_o|$. ^{b} $R_w = [\sum w(|F_o| - |F_c|)^2/\sum w|F_o|^2]^{1/2}$.

diphosphines dramatically influenced the structure of platinum clusters.[16-18] Here, indenyl ligand was used instead of diphosphines to develop routes that produce a cluster-type compound in a stepwise fashion. We wish to report the synthesis and characterization of binuclear palladium complexes of isocyanide with novel bridging η^3-indenyl groups and their transformation to a tetranuclear palladium cluster. A preliminary account of this work has already appeared.[19]

Experimental Section

Benzene and hexane were distilled over calcium hydride prior to use. Other reagents were of the best commercial grade and were used without further purifications. Isocyanide[20] and $PdCl_2(RNC)_2$[21] were prepared by the known methods. All manipulations were carried out under a nitrogen atmosphere.

NMR spectroscopy was carried out on a JEOL GX-400 instrument at room temperature. ^{1}H NMR spectra were measured at 400 MHz in $CDCl_3$ or CD_2Cl_2, and ^{13}C NMR spectra were measured at 100 MHz in CD_2Cl_2. The two-dimensional heteronuclear shift-correlated spectrum (C–H COSY) was recorded by means of the JEOL PLEXUS software (VCHSHF mode). Infrared and electronic absorption spectra were recorded with Jasco A-100 and Ubest-30 spectrometers, respectively.

Preparation of $Pd_2(\mu\text{-}\eta^3\text{-In})_2(RNC)_2$ (3). A suspension of $PdCl_2(RNC)_2$ (R = ^{t}Bu, 2,6-$Me_2C_6H_3$, 2,4,6-$Me_3C_6H_2$, 2,4,6-$^t Bu_3C_6H_2$) (0.50 mmol, 170–360 mg) in 20 mL of benzene was treated at 0 °C dropwise with lithium indenyl (1.0 mmol in 20 mL of THF). The reaction mixture was warmed to room tempertaure and stirred for 1 h. The solvent was removed in vacuo, and the residue was extracted with benzene. The dark red solution was chromatographed on alumina (deactivated by 10 wt % of H_2O) and eluted with benzene. The yellow eluate was concentrated to about 10 mL, and an addition of hexane gave yellow crystals of **3**, which were recrystallized from a benzene–hexane or a dichloromethane–hexane mixed solvent. $Pd_2(\mu\text{-}\eta^3\text{-In})_2(^t BuNC)_2 \cdot {}^1/_2C_6H_6$ (**3a**): Yield 70% (113 mg). Anal. Calcd for $C_{28}H_{32}N_2Pd_2 \cdot {}^1/_2C_6H_6$: C, 57.42; H, 5.44; N, 4.32. Found: C, 56.74; H, 5.55; N, 4.12. IR (Nujol): $\nu_{N\equiv C}$ 2129 s, 2045 sh cm^{-1}. UV–vis (CH_2Cl_2): λ_{max} (log ϵ) 412 (4.18), 309 (4.18) nm. ^{1}H NMR (CD_2Cl_2): δ 1.72 (s, ^{t}Bu), 4.27 (t, H2-In, J = 3.6 Hz), 6.09 (d, H1,3-In, J = 3.6 Hz), 6.74, 7.19 (AA′BB′, H5–8-In). ^{13}C NMR (CD_2Cl_2): δ 31.20 (CH_3-^{t}Bu), 47.76 (C1,3-In), 57.35 (C-^{t}Bu), 89.50 (C2-In), 121.06, 121.72 (C5–8-In), 121.47 (C4,9-In), 142.53 (N≡C). $Pd_2(\mu\text{-}\eta^3\text{-In})_2(2,6\text{-}Me_2C_6H_3NC)_2$ (**3b**): Yield 62% (110 mg). Anal. Calcd for $C_{36}H_{32}N_2Pd_2$: C, 61.29; H, 4.57; N, 3.97. Found: C, 60.40; H, 4.53; N, 3.94. IR (Nujol): $\nu_{N\equiv C}$ 2127, 2108 s cm^{-1}. UV–vis (CH_2Cl_2): λ_{max} (log ϵ) 418 (4.19), 280 (4.78) nm. ^{1}H NMR (CD_2Cl_2): δ 2.67 (s, o-CH_3), 4.38 (t, H2-In, J = 3.7 Hz), 6.32 (d, H1,3-In, J = 3.7 Hz), 6.7–7.3 (m, H-arm). ^{13}C NMR (CD_2Cl_2): δ 19.69 (o-CH_3), 48.11 (C1,3-In), 91.00 (C2-In), 121.63, 122.07 (C5–8-In), 121.83 (C4,9-In), 142.75 (N≡C). $Pd_2(\mu\text{-}\eta^3\text{-In})_2(2,4,6\text{-}Me_3C_6H_2NC)_2$ (**3c**): Yield 51% (94 mg). Anal. Calcd for $C_{38}H_{36}N_2Pd_2$: C, 62.22; H, 4.95; N, 3.82. Found: C, 62.31; H, 4.92; N, 3.92. IR (Nujol): $\nu_{N\equiv C}$ 2135, 2112 s cm^{-1}. UV–vis (CH_2Cl_2): λ_{max} (log ϵ) 417 (4.17), 282 (4.77 nm. ^{1}H NMR (CD_2Cl_2): δ 2.38 (s, p-CH_3), 2.67 (s, o-CH_3), 4.42 (t, H2-In, J = 2.8 Hz), 6.32 (d, H1,3-In, J = 2.8 Hz), 6.6–7.3 (m, H-arm). $Pd_2(\mu\text{-}\eta^3\text{-In})_2(2,4,6\text{-}{}^t Bu_3C_6H_2NC)_2 \cdot CH_2Cl_2$ (**3d**): Yield 16% (43 mg). Anal. Calcd for $C_{56}H_{72}N_2Pd_2 \cdot CH_2Cl_2$: C, 63.93, H, 6.96; N, 2.62. Found: C, 63.96; H, 7.25; N, 2.74. IR (Nujol): $\nu_{N\equiv C}$ 2105 s cm^{-1}. UV–vis (CH_2Cl_2): λ_{max} (log ϵ) 417 (4.05), 284 (4.75) nm. ^{1}H NMR (CD_2Cl_2): δ 1.40 (s, p-^{t}Bu), 1.79 (s, o-^{t}Bu), 4.13 (br, H2-In), 6.40 (br, H1,3-In), 6.7–7.5 (m, H-arm).

Preparation of $Pd_4(\mu\text{-}OAc)_4(\mu\text{-}RNC)_4$ (5). A solution of **3** (0.30 mmol, ca. 200 mg) in 20 mL of benzene was treated at 0 °C dropwise with acetic acid (0.60 mmol (36 mg) in diethyl ether). The reaction mixture was warmed to room temperature and stirred for 48 h. The solution was concentrated to about 10 mL, and an addition of hexane gave yellow crystals of **5**, which were recrystallized from a benzene–hexane mixed solvent. $Pd_4(\mu\text{-}OAc)_4(\mu\text{-}{}^t BuNC)_4 \eta C_6H_6$ (**5a**): Yield 54% (87 mg). Anal. Calcd for $C_{28}H_{48}N_4Pd_4O_8 \cdot C_6H_6$: C, 38.08; H, 5.08; N, 5.22. Found: C, 37.81; H, 5.05; N, 5.20. IR (Nujol): $\nu_{N\equiv C}$ 2075 sh, 2017 s, ν_{RCOO} 1593 s, cm^{-1}. UV–vis (CH_2Cl_2): λ_{max} (log ϵ) 312 (3.63) nm. ^{1}H NMR ($CDCl_3$): δ 1.48 (s, ^{t}Bu), 1.92 (s, CH_3COO). $Pd_4(\mu\text{-}OAc)_4(\mu\text{-}2,6\text{-}Me_2C_6H_3NC)_4$ (**5b**): Yield 43% (77 mg). Anal. Calcd for $C_{44}H_{48}N_4Pd_4O_8$: C, 44.54; H, 4.08: N, 4.72. Found: C, 45.25, H, 3.73; N, 4.49. IR (Nujol): $\nu_{N\equiv C}$ 2007 sh, 1976 s, ν_{RCOO} 1571 s cm^{-1}. UV–vis (CH_2Cl_2): λ_{max} (log ϵ) 312 (3.63) nm. ^{1}H NMR ($CDCl_3$): δ 1.67 (s, CH_3COO), 2.42 (s, o-CH_3).

Crystal Data and Intensity Measurements for $Pd_2(\mu\text{-}\eta^3\text{-In})_2(^t BuNC)_2$ (3a), $Pd_2(\mu\text{-}\eta^3\text{-In})_2(2,6\text{-}Me_2C_6H_3NC)_2$ (3b), and $Pd_4(\mu\text{-}OAc)_4(\mu\text{-}{}^t BuNC)_4 \cdot C_6H_6$ (5a). Crystal data and experimental conditions for **3a**, **3b**, and **5a** are listed in Table I. Yellow crystals of **3a**, **3b**, and **5a** sealed into a 0.7-mm i.d. glass-tube capillary were used in the intensity data collection on a Rigaku four-circle automated diffractometer AFC5S (**3a**, **5a**) and a Enraf-Nonius CAD4 (**3b**) equipped with Mo Kα radiation. Three standard reflections were monitored every 150 reflections for each compounds and showed no systematic decrease in intensity. Totals of 1930 reflections (**3a**), 3250 reflections (**3b**), and 2413 reflections (**5a**) were measured, and the intensities were corrected for Lorentz–polarization effects. Absorption corrections were applied.

Structure Solution and Refinement. Compound 3a. The structure was solved by direct methods with MITHRIL.[22] The two palladium atoms were located in the initial E map, and subsequent Fourier syntheses gave the positions of other non-hydrogen atoms. Hydrogen atoms were calculated at the ideal positions, with the C–H distance of 0.95 Å, and were not refined. The structure was refined with full-matrix least-squares techniques. Final refinement with anisotropic thermal parameters for non-hydrogen atoms converged to R = 0.061 and R_w = 0.049, where $R = \sum\|F_o| - |F_c\|/\sum|F_o|$ and $R_w = [\sum w(|F_o| - |F_c|)^2/\sum w|F_o|^2]^{1/2}$ ($w = 1/\sigma^2(F_o)$). A final difference Fourier synthesis showed peaks at heights up

(17) Tanase, T.; Kudo, Y.; Ohno, M.; Kobayashi, K.; Yamamoto, Y. *Nature* **1990**, *344*, 526.
(18) Tanase, T.; Horiuchi, T.; Yamamoto, Y.; Kobayashi, K. *J. Organomet. Chem.* **1992**, *440*, 1.
(19) Tanase, T.; Nomura, T.; Yamamoto, Y.; Kobayashi, K. *J. Organomet. Chem.* **1991**, *410*, C25.
(20) (a) Walborsky, H. M.; Nizwk, G. E. *J. Org. Chem.* **1972**, *37*, 187. (b) Yamamoto, Y.; Aoki, K.; Yamazaki, H. *Inorg. Chem.* **1979**, *18*, 1681.
(21) Bonati, F.; Minghetti, G. J. *J. Organomet. Chem.* **1970**, *24*, 251.
(22) Gilmore, G. J. *J. Appl. Crystallogr.* **1984**, *17*, 42.

to 1.1 e Å^{-3} around the Pd(1) atom. Atomic scattering factors and values of f' and f'' for Pd, Cl, P, F, N, and C were taken from refs 23 and 24. All calculations were carried out on a Digital VAX Station 3100 M38 with the TEXSAN–TEXRAY Program System. The perspective views were drawn by using the program ORTEP.[25]

Compound 3b. The structure was solved by direct methods with MULTAN78.[26] The two palladium atoms were located in the initial E map, and subsequent Fourier syntheses gave the positions of other non-hydrogen atoms. The coordinates of all hydrogen atoms were calculated at the ideal positions. The structure was refined with block-diagonal least-squares techniques. Final refinement with anisotropic thermal parameters for non-hydrogen atoms (hydrogen atoms were not refined) converged to $R = 0.059$ and $R_w = 0.070$ ($w = 1$). A final difference Fourier synthesis showed peaks at heights up to 0.83 e Å^{-3} around the Pd atom. All calculations were carried out on a FACOM M-780 computer at the Computer Center of the Institute of Physical and Chemical Research with the Universal Crystallographic Computing Program System UNICS III.[27]

Compound 5a. The structure was solved by direct methods with MITHRIL. The three palladium atoms were located in the initial E map, two of which occupy special position m with the occupancy of 0.5, and subsequent Fourier syntheses gave the positions of other non-Hydrogen atoms. Hydrogen atoms were not located, because of the large thermal factors of methyl carbons. The structure was refined with full-matrix least-squares techniques. Final refinement with anisotropic thermal parameters for non-hydrogen atoms (the carbon atoms of the *tert*-butyl groups and the benzene molecule were refined isotropically) converged to $R = 0.061$ and $R_w = 0.064$, where $R = \sum||F_o| - |F_c||/\sum|F_o|$ and $R_w = [\sum w(|F_o| - |F_c|)^2/\sum w|F_o|^2]^{1/2}$ ($w = 1/\sigma^2(F_o)$). A final difference Fourier synthesis showed peaks at heights up to 1.20 e Å^{-3} around the solvated benzene molecule.

Molecular Orbital Calculations. The calculations were of the extended Hückel type using parameters of the Coulomb integrals, and the orbital exponents were taken from ref 28. For the Pd d functions, a double-ζ expansion was used. Geometrical assumptions were derived from the crystal structures of **3b** and **5** (molecule A).

Results and Discussion

Preparation of $Pd_2(\mu\text{-}\eta^3\text{-In})_2(RNC)_2$ (3). A slurry of $PdCl_2(RNC)_2$ in benzene was treated at 0 °C dropwise with an excess of lithium indenyl (LiIn), and the mixture was stirred at room temperature for 1 h. The resultant dark red solution was chromatographed on deactivated alumina to afford yellow crystals formulated as $Pd_2(In)_2(RNC)_2$ (**3a**, R = ^{t}Bu; **3b**, R = 2,6-$Me_2C_6H_3$; **3c**, R = 2,4,6-$Me_3C_6H_2$; **3d**, R = 2,4,6-$^t Bu_3C_6H_2$). The yield of **3d** was fairly low (16%) compared with those of **3a–c** (51–70%), presumably because of steric bulk of isocyanide ligands. The compounds **3** are stable in benzene but slowly decomposed in halogen-containing hydrocarbons even under a nitrogen atmosphere. Complex **3b** could also be prepared by the reaction of palladium(I) dimer $Pd_2Cl_2(XylNC)_4$ with LiIn, but the yield was suppressed to 15% owing to the deposition of elemental palladium. The IR spectra of **3** showed peaks around 2100 cm^{-1} corresponding to the terminal isocyanides ($\nu_{N\equiv C}$). The frequency of $\nu_{N\equiv C}$ decreased by ca. 100 cm^{-1} from those of parent palladium(II) complexes, indicating that the metal center was reduced to monovalent state. The UV–vis spectra exhibited an absorption at 418 nm, assignable to the σ–σ^* transition for a metal–metal bond by analogy with those of other palladium(I) dimers.[10,11,29,30]

The ^{1}H NMR spectra showed the presence of one kind of isocyanide and indenyl groups. In the ^{1}H NMR spectrum of **3a**, an AX_2 pattern for the five-membered indenyl ring protons was observed at δ 4.27 (t, H2, J = 3.6 Hz) and 6.09 (d, H1,3, J = 3.6 Hz), and an AA′BB′ system for the benzenoid ring protons at δ 6.74 and 7.19.[31] The resonance for ^{t}Bu groups of isocyanides was observed as a singlet at δ 1.72. The ^{13}C NMR spectrum of **3a** showed three peaks of the five-membered ring carbons at δ 47.76 (C1,3), 89.50 (C2), and 121.47 (C4,9), together with a signal for N≡C carbons of isocyanides at δ 142.53. The assignment was confirmed by ^{13}C–^{1}H COSY spectrum as shown in Figure 1.[32] It is known that ^{1}H and ^{13}C NMR spectroscopy is very effective for determining the hapticity of an indenyl group coordinated to a monometallic center.[2] On going from η^5 to η^3 coordination, the resonance for the H1,3 protons undergoes a large upfield shift, while the resonance for the H2 proton undergoes a downfield shift, e.g. from δ 4.89 (H1,3) and 5.82 (H2) for Ir(η^5-In)$(C_8H_{14})_2$[5] to δ 2.77 (H1,3) and 7.09 (H2) for Ir(η^3-In)$(PMe_3)_2$[5] and from δ 4.5 (H1,3) and 5.6 (H2) for Fe(η^5-In)$(CO)_2$R (R = alkyl)[33] to δ 3.54 (H1,3) and 7.6 (H2) for $[(PPh_3)_2N][Fe(\eta^3\text{-In})(CO)_3]$.[6] The chemical shift of the C4 and C9 ring-junction carbons in ^{13}C NMR spectrum is also a good indication of η^3-bonding mode, which is usually shifted to downfield by ca. 40 ppm from those of η^5-indenyl groups. However, the chemical shifts for H1,3 and C4,9 resonances of **3** did not fall within the region described above, and those for H2 and C1,3 showed unusual upfield shifts, suggesting that the coordination system of indenyl groups is not the normal η^5- or η^3-type bound to a mononuclear center. (It was shown to be a bridging η^3-indenyl from the X-ray crystallographic analyses (*vide infra*).) As to the palladium and platinum complexes of η^3-indenyl groups, the split between H1,3 and H2 proton resonances is not so large; the peak for the H1–3 protons appeared at δ 6.69 for Pt(η^5-In)(C_8H_{12}),[34] and those for H1,3 and H2 protons of $Pd_2(\mu\text{-Cl})_2(\eta^3\text{-In})_2$[28] were observed at δ 6.30 and 6.69, respectively.

When $PdCl_2(PPh_3)_2$ and $[^nBu_4N][PdCl_3(CO)]$ were used as starting complexes, any dipalladium compounds with bridging η^3-indenyl groups like **3** were not obtained. Thus, the bridging structure with η^3-indenyl ligands could be unique to the isocyanide complexes.

Crystal Structures of $Pd_2(\mu\text{-}\eta^3\text{-In})_2(^t BuNC)_2$ (3a) and $Pd_2(\mu\text{-}\eta^3\text{-In})_2(2,6\text{-}Me_2C_6H_3NC)_2$ (3b). In order to clarify the coordination mode of indenyl groups, X-ray crystallographic analyses of **3a,b** were undertaken. The molecular structure of **3a** with the atomic numbering scheme is shown in Figure 2a, and some selected bond lengths and angles are listed in Table II. The molecule of **3a** consists of two palladium atoms almost symmetrically bridged by two indenyl groups. The molecule has no crystallographically imposed symmetry, but its ideal symmetry is C_{2v}. The arrangement of the two indenyl ligands is entirely different from $Pd_2(\mu\text{-}\eta^3\text{-Cp})_2(PEt_3)_2$ (**1a**), in which two Cp planes are parallel in an *anti* arrangement and the $Pd_2(PEt_3)_2$ unit is almost linear (the Pd–Pd–P angle (τ) is 175.45(4)°). In complex **3a**, the two indenyl planes lie in a wedge-shaped array in a *syn* arrangement (Figure 3a). The dihedral angle (ϕ) between the two indenyl planes is 66.5°, being tentatively derived from the repulsion between the two indenyl benzenoid rings. Further, the average Pd–Pd–C_{RNC} angle (τ) is 153.0°, showing a distortion from the C–Pd–Pd–C linear structure to an A-frame one (Figure

(23) Cromer, D. T.; Waber, J. T. *International Tables for X-ray Crystallography*; Kynoch Press: Birmingham, England, 1974; Vol. IV.
(24) Cromer, D. T. *Acta Crystallogr.* **1965**, *18*, 17.
(25) Johnson, C. K. *ORTEPII*. Oak Ridge National Laboratory, Oak Ridge, TN, 1976.
(26) Main, P.; Lessinger, L.; Woolfson, M. M.; Germain, G.; Declerq, J. P. MULTAN78. Universities of York, England, and Louvain, Belgium, 1978.
(27) Sakurai, T.; Kobayashi, K. *Rikagaku* Kenkyusho *Hokoku* **1979**, *55*, 69.
(28) Nakasuji, K.; Yamaguchi, M.; Murata, I.; Tatsumi, K.; Nakamura, A. *Organometallics* **1984**, *3*, 1257.
(29) Holloway, R. G.; Penfold, B. R.; Colton, R.; McCormick, M. J. *J. Chem. Soc., Chem. Commun.* **1976**, 485.
(30) Kullberg, M. L.; Lemke, F. R.; Powell, D. R.; Kubiak, C. P. *Inorg. Chem.* **1985**, *24*, 3589.

(31) The notation H1–9 and C1–9 represents the standard numbering of indenyl group shown as

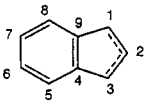

(32) Supplementary material.
(33) Forschner, T. C.; Cutler, A. R. *Inorg. Chim. Acta* **1985**, *102*, 113.
(34) O'Hare, D. *Organometallics* **1987**, *6*, 1766.

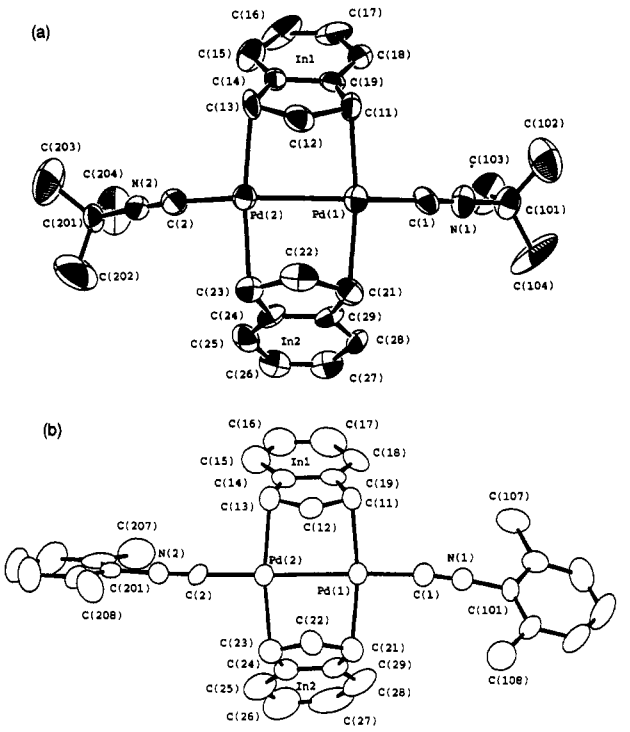

Figure 2. Perspective drawings of (a) $Pd_2(\mu\text{-}\eta^3\text{-In})_2(^t\text{BuNC})_2$ (**3a**) and (b) $Pd_2(\mu\text{-}\eta^3\text{-In})_2(\text{XylNC})_2$ (**3b**).

3a). The palladium–palladium bond length of 2.648(2) Å falls within the range of Pd(I)–Pd(I) single bonds and is fairly longer than those found in unbridged palladium(I) dimers, e.g. $Pd_2Cl_2(^t\text{BuNC})_4$ (2.532(2) Å)[10] and $[Pd_2(\text{MeNC})_6](PF_6)_2$ (2.531(9) Å),[35,36] and shorter than those of $Pd_2(\mu\text{-}\eta^3\text{-Cp})_2(PEt_3)_2$ (**1a**) (2.673(1) Å)[7] and $Pd_2Cl_2(\mu\text{-dppm})_2$ (2.699(2) Å).[29] An average bond length between the Pd atoms and the C1 and C3 carbon atoms is 2.19 Å, and that between the Pd atoms and the C2 apex carbon atoms is 2.46 Å.[31] The apex carbon atoms almost symmetrically interact with the both Pd atoms. The average distance between the Pd atoms and ring-junction carbon atoms (r_{MCj}) is 3.08 Å, which is clearly out of the normal bonding range. These structural parameters indicate the η^3-allyl–ene bonding mode of indenyl groups. The C–C bond lengths in the five-membered rings also show evidence of an allyl–ene distortion. It should be noted that, despite the extreme slippage to η^3-allyl–ene bonding, the distortion of the indenyl groups from planarity is very small. The average fold angle (θ) between the η^3-allyl plane and the benzenoid ring is 10°, in contrast to that of 26° for $W(\eta^5\text{-In})(\eta^3\text{-In})(CO)_2$,[3] 28° for $Ir(\eta^3\text{-In})(PMe_2Ph)_3$,[5] and 22° for $[Fe(\eta^3\text{-In})(CO)_3]^-$.[6] However, it is comparable to that of 12° for $V(\eta^5\text{-In})(\eta^3\text{-In})(CO)_2$,[4] showing that the fold angle is not necessarily a good indication of η^3-slippage for indenyl groups. As to the bridging indenyl groups, the average distance of metal–ring-junction carbon (r_{MCj}) seems to be a reliable parameter for η^3-distortion, from which the distortion toward η^3-mode in **3a** is more significant than is found in the Cp analogue of **1a** (r_{MCj} = 2.85 Å). The terminal isocyanides are almost linear with an average Pd–C–N angle of 174°, average C–N–C angle of 178°, an average Pd–C_{RNC} bond length of 1.96 Å, and an average N≡C bond length of 1.16 Å.

The molecular structure of **3b** with the atomic numbering scheme is shown in Figure 2b, and some selected bond lengths and angles are listed in Table II. The structure of **3b** is isomorphous to that of **3a**. Structural parameters are summarized in Table III. The Pd–Pd bond length of 2.656(2) Å is slightly longer than that of **3a**, and the average Pd–Pd–C_{RNC} angle of 163.7° is larger by ~10° than that found in **3a**. It was presumed that a *trans*-effect of the terminal isocyanides influenced the length of the Pd–Pd bond, and its degree is estimated to increase with increasing the Pd–Pd–C_{RNC} angle (τ). In fact, the order of Pd–Pd bond distances in **3a**, **3b**, and **1a** is in accordance with the order of the τ angles. The dihedral angle ϕ and the average fold angle θ are 48.3 and 7°, respectively, and both of which are smaller than those in **3a**.

From these crystal structures, the dipalladium complex **3** is revealed to have a novel wedge-shaped structure where two η^3-indenyl groups bridged across the two palladium atoms in a *syn* arrangement. To our knowledge, this is the first isolated example in which η^3-indenyl groups act as bridging ligands.

Molecular Orbital Descriptions for 3. To understand the electronic structure of the compound **3**, extended Hückel MO calculations were carried out on a model of *syn*-$Pd_2(\mu\text{-}\eta^3\text{-In})_2(HNC)_2$ (**4**) (θ = 0°, ϕ = 0°, τ = 0°, and Pd–Pd = 2.65 Å). An interaction diagram for **4** is given in Figure 4. The HOMO is mainly derived from an antibonding interaction of the occupied σ_d orbital of $[Pd_2(HNC)_2]^{2+}$ with the occupied a_1 orbital of indenyl anions, and the LUMO is mainly from a repulsive interaction of the empty σ_d* orbital of the Pd_2 unit with the occupied b_1 orbital of indenyl anions. The δ_d and δ_d* orbitals of the Pd_2 unit are mixed into the HOMO and the LUMO in an antibonding manner, respectively. The energy gap between the HOMO and the LUMO is sufficiently large to adopt the spin-paired singlet state, resulting in a Pd–Pd single bond. The diamagnetism of **3** supported this energy profile. The major energy gain on combining the $[Pd_2(HNC)_2]^{2+}$ and the *syn*-In_2^{2-} units orginates from a bonding interaction between the σ_d* orbital of the Pd_2 unit and the b_1 orbital of the indenyl anions, but it is rather unstabilized by an *anti*-bonding interaction with the occupied δ_d* orbital of the Pd_2 fragment. This energy gain is relatively small compared with the corresponding gain (b_2(Pd) – $2a_2$(In)) in the mononuclear model of $Pd(\eta^3\text{-In})(acac)$.[28] The electronic advantage responsible for the wedge-shaped arrangement as observed in **3** was not elucidated from the present EHMO calculations.

Reactions of 3. The isolated palladium(I) dimer of **3** was exclusively the *syn*-isomer (*syn*-**3**), and the possible *anti*-isomer

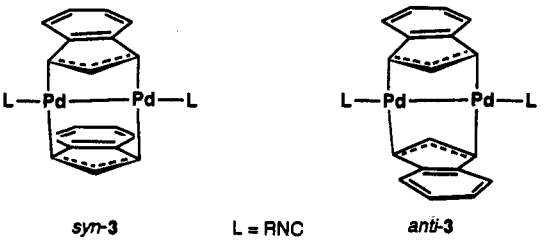

was not obtained. In order to examine the presence of the *anti*-isomer, the ^{1}H NMR spectrum of the reaction mixture of **3a**, just after a purification on alumina, was measured at room temperature (Figure 5).[32] Besides the major peaks for *syn*-**3a**, a set of minor peaks assigned to the *anti*-isomer were observed, the resonance for the H2 proton of indenyl groups undergoing further upfield shift owing to the ring-current influence of benzenoid rings. The ratio of *syn*/*anti* isomers was estimated at ca. 8:2 from the intensities of methyl protons. It is notable that the *syn*- and *anti*-isomers were not equilibrated even at 60 °C.

The reactions of **3a** with CO, PPh_3, ^{t}BuNC, PhSH, and HBF_4 at room temperature resulted in the deposition of palladium metal. The reaction of **3a** with I_2 gave $PdI_2(^t\text{BuNC})_2$ in a 36% yield. These results showed that the reactivity of **3** is quite different from that of the Cp analogue **1** and that the bridging η^3-indenyl groups are readily dissociated from the metal centers. When **3a** was treated with acetic acid in benzene for 48 h, yellow crystals

(35) (a) Doonan, D. J.; Balch, A. L.; Goldberg, S. Z.; Eisenberg, R.; Miller, J. S. *J. Am. Chem. Soc.* **1975**, *97*, 1961. (b) Goldberg, S. Z.; Eisenberg, R. *Inorg. Chem.* **1976**, *15*, 535.

(36) Miller, T. D.; Clair, M. A. St.; Reinking, M. K.; Kubiak, C. P. *Organometallics* **1983**, *2*, 767.

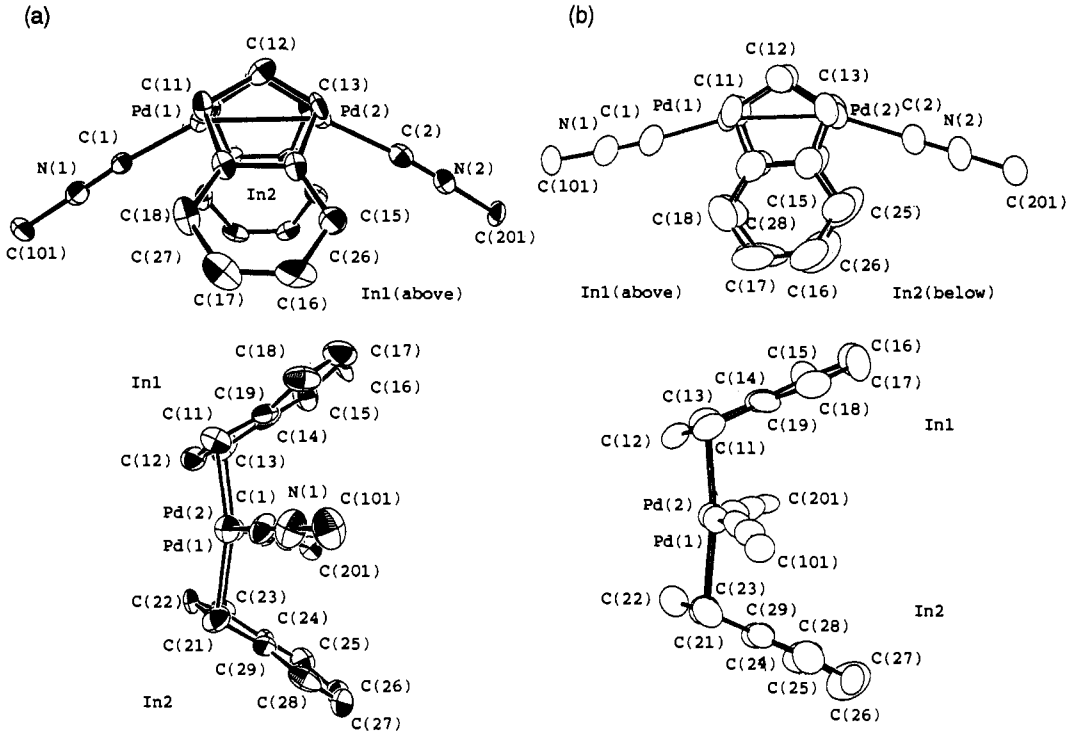

Figure 3. Perspective drawings of (a) $Pd_2(\mu\text{-}\eta^3\text{-In})_2(^t\text{BuNC})_2$ (**3a**) and (b) $Pd_2(\mu\text{-}\eta^3\text{-In})_2(\text{XylNC})_2$ (**3b**), showing the A-frame structure and the wedge-shaped arrangement.

Table II. Selected Bond Distances (Å) and Angles (deg) of **3a,b**[a]

	3a	**3b**
	Bond Distances	
Pd(1)–Pd(2)	2.648(2)	2.656(2)
Pd(1)–C(1)	1.95(2)	1.96(1)
Pd(2)–C(2)	1.97(2)	1.95(1)
Pd(1)–C(11)	2.17(2)	2.16(1)
Pd(1)–C(21)	2.20(2)	2.17(2)
Pd(2)–C(13)	2.20(2)	2.19(2)
Pd(2)–C(23)	2.19(2)	2.18(2)
Pd(1)–C(12)	2.46(2)	2.52(1)
Pd(2)–C(12)	2.43(2)	2.50(1)
Pd(1)–C(22)	2.47(2)	2.52(2)
Pd(2)–C(22)	2.48(2)	2.49(1)
Pd(1)–C(19)	3.05(2)	3.01(1)
Pd(1)–C(29)	3.07(1)	3.00(1)
Pd(2)–C(14)	3.13(2)	2.99(1)
Pd(2)–C(24)	3.07(1)	3.03(2)
N(1)–C(1)	1.16(2)	1.15(2)
N(2)–C(2)	1.16(2)	1.16(2)
N(1)–C(101)	1.43(2)	1.41(2)
N(2)–C(201)	1.44(2)	1.41(2)
	Bond Angles	
Pd(2)–Pd(1)–C(1)	152.2(5)	165.8(4)
Pd(1)–Pd(2)–C(2)	153.8(5)	161.6(4)
Pd(2)–Pd(1)–C(11)	85.9(4)	85.7(4)
Pd(2)–Pd(1)–C(21)	86.2(4)	85.0(4)
Pd(1)–Pd(2)–C(13)	85.8(4)	85.5(4)
Pd(1)–Pd(2)–C(23)	85.9(4)	86.0(4)
Pd(1)–C(1)–N(1)	175(2)	174(1)
Pd(2)–C(2)–N(2)	173(1)	178(1)
C(1)–N(1)–C(101)	179(2)	174(1)
C(2)–N(2)–C(201)	177(2)	179(1)

[a] Estimated standard deviations in parentheses.

Table III. Structural Parameters of the Complexes **3a,b**

	3a		**3b**	
	In1	In2	In1	In2
dihedral angle θ ([In1] vs [In2]), deg	66.5		48.3	
fold angle ϕ ([C_3] vs [C_6]), deg	10.5	10.2	5.0	7.7
av C1–C2, C2–C3 bond length, Å	1.40	1.42	1.41	1.41
av C1–C9, C3–C4 bond length, Å	1.48	1.44	1.49	1.47
av C–C bond length in benzenoid ring, Å	1.38	1.39	1.40	1.40
av Pd–Pd–C_{RNC} bond angle τ, deg	153.0		163.7	
av Pd–C1,3 bond length, Å	2.19		2.17	
av Pd–C2 bond length, Å	2.46		2.51	
av Pd···C4,9 distance, Å	3.08		3.01	

formulated as $[Pd(OAc)(^t\text{BuNC})]_n$ (**5a**) were obtained in a yield of 54%. A similar compound of $[Pd(OAc)(2,6\text{-}Me_2C_6H_3NC)]_n$ (**5b**) was also prepared by a treatment of **3b** with acetic acid (43%). The ^{1}H NMR spectra of **5** indicated the presence of one kind of isocyanide and acetate group, and the IR spectra showed an intense absorption around 2000 cm^{-1}, which falls within the range corresponding to bridging isocyanides with a linear C–N–C form (*vide infra*).[11] In order to clarify the structure, an X-ray crystallographic analysis for **5a** was undertaken.

Crystal Structure of $Pd_4(\mu\text{-}OAc)_4(\mu\text{-}^t\text{BuNC})_4\cdot C_6H_6$ (5a). Half of the unit cell consists of two independent cluster molecules and two solvated benzene molecules. Perspective drawings of the two cluster molecules (A and B) with the atomic numbering scheme are shown in Figure 6, and selected bond lengths and angles are given in Table IV. The cluster molecules A and B have almost identical structures except for a slight difference of the Pd_4 frameworks.

Cluster A is composed of tetranuclear palladium atoms and four isocyanides and four acetate ligands and has a crystallo-

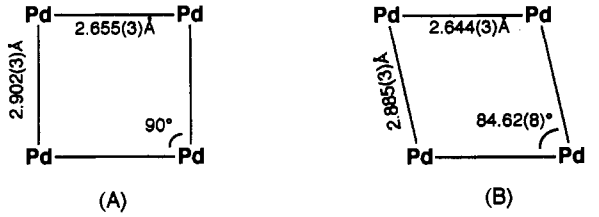

graphically imposed C_2 axis along the *b* axis of the unit cell and a mirror plane perpendicular to the C_2 axis; the N(1), N(2), C(1), C(2), C(11), C(13), C(21), and C(23) atoms are in the mirror plane. The Pd_4 framework is rectangular with the short Pd–Pd bonds (Pd(1)–Pd(1)* = 2.655(3) Å) bridged by two

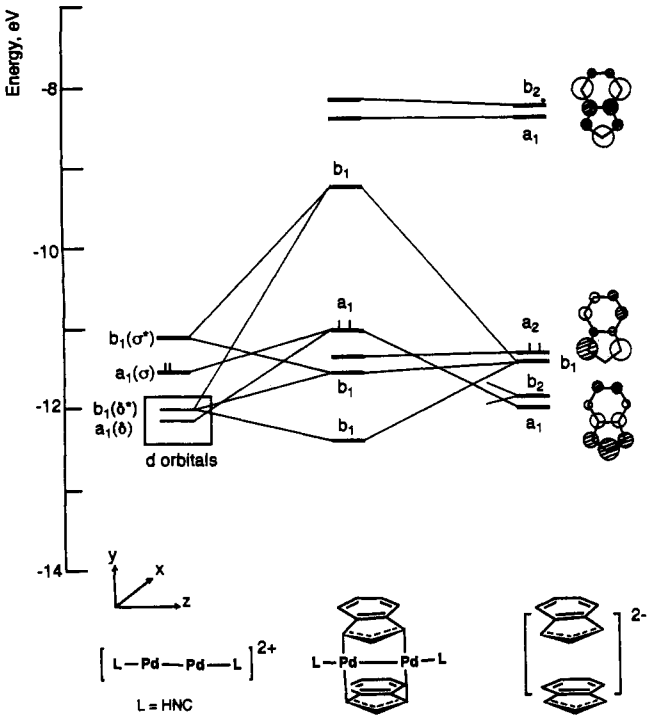

Figure 4. Interaction diagram for the valence orbitals of $Pd_2(\mu$-η^3-In$)_2$-(HNC)$_2$ (**4**).

isocyanides and the long Pd–Pd interactions (Pd(1)–Pd(1)** = 2.902(3) Å) bridged by two acetate anions. The former length is comparable to that of $Pd_2Cl_2(\mu$-2,6-$Me_2C_6H_3NC)_2$(pyridine)$_2$ (**6**) (2.662(1) Å)[11] and falls within the range reported for Pd–Pd bonds in palladium(I) complexes.[30] The latter distance is longer than the Pd–Pd bond length in the metal (2.751 Å)[37] and is noticeably shorter than twice the covalent radius of Pd (2.98 Å).[38] The interaction between the Pd(1) and Pd(1)* atoms might be very weak, and the long distance of 2.902(3) Å seems to be attributable to the five-membered ring size of acetate anion. A similar Pd–Pd distance (2.94 Å) was found in $Pd_2(\eta$-$C_3H_5)_2(\mu$-OAc$)_2$[39] where [Pd(η-C_3H_5)]$^+$ fragments are connected by acetate ligands.

The coordination geometry around the Pd atoms is square planar (ignoring the metal–metal bond); the C(1)–Pd(1)–C(2) angle is 88.6(7)°, and the O(1)–Pd(1)–O(2) angle is 89.3(4)°. The five-membered chelate ring comprised of acetate ligand is planar, and the two Pd_2(OAc) planes are almost perpendicular. The Pd(1)**–Pd(1)–O(1) and Pd(1)*–Pd(1)–O(2) angles are 79.6(3) and 82.0(3)°. The two isocyanides are symmetrically bridged between the Pd(1) and Pd(1)* atoms with an average Pd–C bond length of 1.99 Å and an average Pd–C–Pd angle of 83.6°. The remarkable feature of the isocyanide ligands is the

Table IV. Selected Bond Distances (Å) and Angles (deg) of **5a**[a]

Bond Distances			
Pd(1)–Pd(1)*	2.655(3)	Pd(2)–Pd(3)	2.664(3)
Pd(1)–Pd(1)**	2.902(3)	Pd(2)–Pd(3)*	2.885(3)
Pd(1)–O(1)	2.16(1)	Pd(2)–O(4)	2.15(1)
Pd(1)–O(2)	2.16(1)	Pd(2)–C(3)	2.00(2)
Pd(1)–C(1)	1.98(2)	Pd(3)–O(3)	2.15(1)
Pd(1)–C(2)	2.00(2)	Pd(3)–C(3)	1.99(2)
N(1)–C(1)	1.16(3)		
N(2)–C(2)	1.16(3)	N(3)–C(3)	1.18(2)
N(1)–C(11)	1.53(4)		
N(2)–C(21)	1.57(4)	N(3)–C(31)	1.46(3)
Bond Angles			
Pd(1)*–Pd(1)–Pd(1)**	90.00	Pd(3)*–Pd(2)–Pd(3)	84.62(8)
Pd(1)*–Pd(1)–O(1)	135.0(3)	Pd(3)–Pd(2)–O(4)	133.5(3)
Pd(1)*–Pd(1)–O(2)	132.7(3)	Pd(2)–Pd(3)–O(3)	133.5(3)
Pd(1)*–Pd(1)–C(1)	48.0(5)	Pd(3)–Pd(2)–C(3)	48.0(5)
Pd(1)*–Pd(1)–C(2)	48.5(4)	Pd(2)–Pd(3)–C(3)	48.2(4)
Pd(1)**–Pd(1)–O(1)	79.6(3)	Pd(3)*–Pd(2)–O(4)	83.1(3)
Pd(1)**–Pd(1)–O(2)	82.0(3)	Pd(2)*–Pd(3)–O(3)	78.3(3)
Pd(1)**–Pd(1)–C(1)	108.6(7)	Pd(3)*–Pd(2)–C(3)	99.9(4)
Pd(1)**–Pd(1)–C(2)	101.6(6)	Pd(2)*–Pd(3)–C(3)	107.3(4)
O(1)–Pd(1)–O(2)	89.3(4)	O(4)–Pd(2)–O(4)*	89.0(6)
O(1)–Pd(1)–C(1)	171.7(7)	O(4)–Pd(2)–C(3)	90.6(5)
O(1)–Pd(1)–C(2)	90.7(6)	O(4)–Pd(2)–C(3)*	176.9(5)
O(2)–Pd(1)–C(1)	90.8(6)	C(3)–Pd(2)–C(3)*	89.6(9)
O(2)–Pd(1)–C(2)	176.4(7)	O(3)–Pd(3)–O(3)*	90.8(6)
C(1)–Pd(1)–C(2)	88.6(7)	O(3)–Pd(3)–C(3)	89.4(5)
		O(3)–Pd(3)–C(3)*	174.2(5)
		C(3)–Pd(3)–C(3)*	89.9(9)
Pd(1)–C(1)–Pd(1)*	84.1(9)	Pd(2)–C(3)–Pd(3)	83.8(7)
Pd(1)–C(2)–Pd(1)*	83.0(9)	Pd(2)–C(3)–N(3)	139(1)
Pd(1)–C(1)–N(1)	138.0(5)	Pd(3)–C(3)–N(3)	137(1)
Pd(1)–C(2)–N(2)	138.5(4)		
C(1)–N(1)–C(11)	171(3)	C(3)–N(3)–C(31)	171(2)
C(2)–N(2)–C(21)	177(3)		

[a] Estimated standard deviations in parentheses. Symmetry operation for the atoms with asterisks are as follows: Pd(1)* (x, $-y$, z), Pd(1)** ($-x+1$, y, $-z+1$), Pd(2)* ($-x+2$, $-y$, $-z$), Pd(3)* ($-x+2$, $-y$, $-z$), O(4)* (x, $-y$, z), C(3)* (x, $-y$, z).

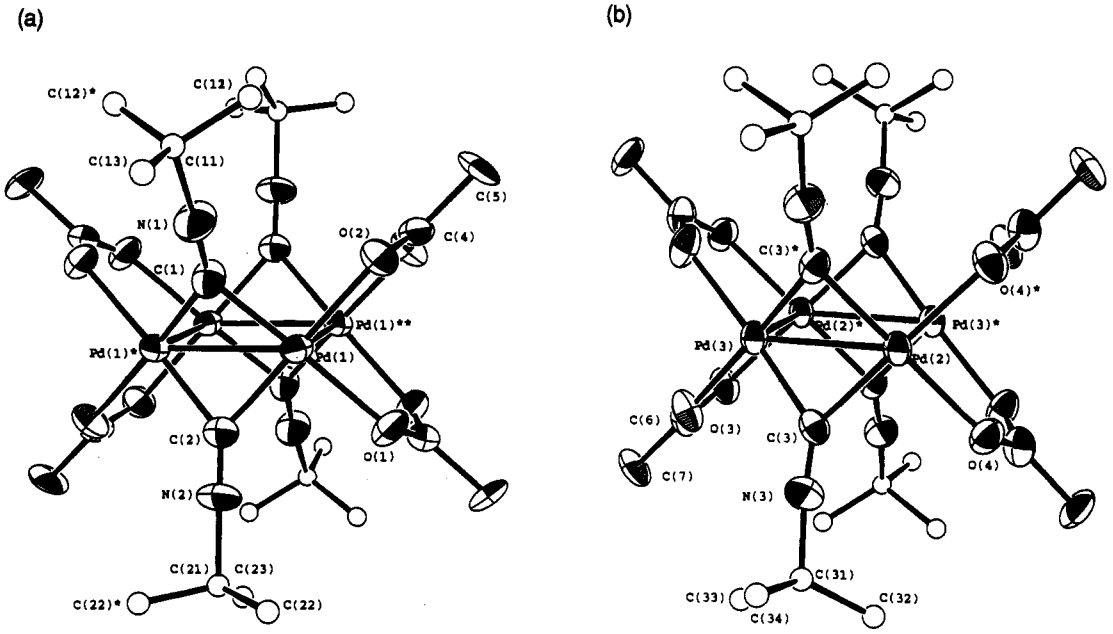

Figure 6. Perspective drawings of $Pd_4(\mu$-OAc$)_4(\mu$-^{t}BuNC$)_4$ (**5a**): (a) molecule A; (b) molecule B.

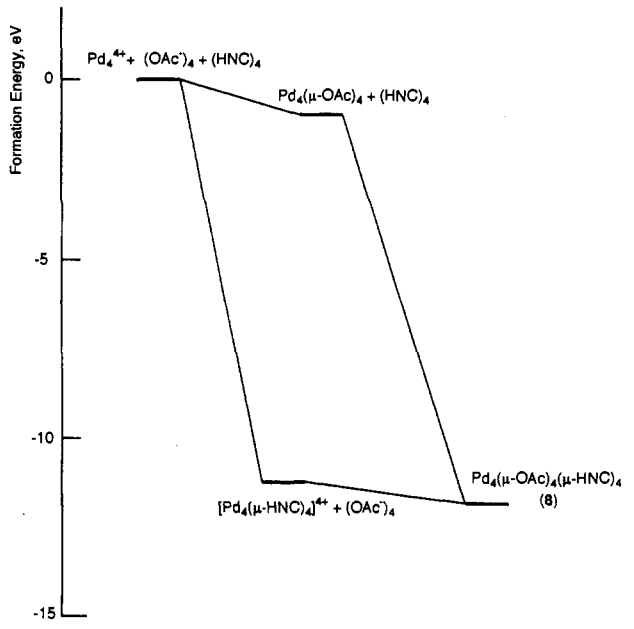

Figure 7. Energy formation diagram for $Pd_4(\mu\text{-}O_2CH)_4(\mu\text{-}HNC)_4$ (**8**).

linear form with the C–N–C bond angles (average 174°) and the short C=N bond distances (average 1.16 Å), suggesting that the back-bonding interaction to the C≡NR moiety is very weak. The bridging behvior of a linear isocyanide was already observed in the dipalladium compound **6**, in which one of the bridging C–N–C angles and the C=N bond lengths are 175° and 1.19 Å, respectively.[11] This C–N triple-bonded character of RNC is responsible for the high frequency of $\nu_{C=N}$ compared with those of usual bridging RNC (1580–1880 cm^{-1}).[40] The Pd_2C_2 core is puckerd with a dihedral angle of 138° between the two Pd_2C planes just as observed in **6** (130°).

The cluster molecule B has a crystallographically imposed C_2 axis along the *b* axis of the unit cell and a mirror plane vertical to the C_2 axis; the Pd atoms are included in the mirror plane. The Pd_4 framework of the molecule B is shaped like a parallelogram (Pd(3)–Pd(2)–Pd(2)* = 84.62(8)°) with the short Pd–Pd bonds (Pd(2)–Pd(3) = 2.644(3) Å) and the long Pd–Pd interactions (Pd(2)–Pd(3)* = 2.885(3) Å). The other structural parameters are almost identical to those of A.

The analogous tetranuclear palladium(I) cluster with the bridging carbonyl groups, $Pd_4(\mu\text{-}OAc)_4(\mu\text{-}CO)_4$ (**7**), has already been reported,[41] and the structural feature is closely similar to the present isocyanide cluster. While the cluster **7** was easily prepared by the reaction of $Pd(OAc)_2$ with CO in acetic acid, the cluster **5** could only be prepared through the indenyl dimer **3**; some attempts by the reaction of $Pd(OAc)_2$ with RNC in the presence of a reducing reagent and that of $Pd_2Cl_2(RNC)_4$ with NaOAc failed in obtaining the cluster **5**.

Molecular Orbital Descriptions for 5. First we chose $[Pd_4(\mu\text{-}O_2CH)_4(\mu\text{-}HNC)_4]$ (**8**) as a model compound for **5**, and the bond angles and distances are idealized as follows. The Pd_4 framework is rectangular with two different Pd–Pd distances (2.66, 2.90 Å), the dihedral angle between the two Pd_2C planes is 138°, and that between the two Pd_2O_2C planes is 90°. Pd–O = 2.16 Å, Pd–C = 2.00 Å, C–N = 1.16 Å, and C–O = 1.24 Å. C–H, N–H = 1.05 Å, Pd–Pd–O = 80°, and C–N–C = 180°. The energy formation diagram is presented in Figure 7, which definitely indicates that the major stabilization energy is generated from the interaction between the Pd_4 core and the bridging HNC groups, and the carboxylate ligands act as only σ-donating ligands. From these, we simplified our model of **8** to $[Pd_2(\mu\text{-}HNC)_2(OH)_4]_2^{4-}$ (**9**) (Pd–Pd–O = 90°), which is composed of two $[Pd_2(\mu\text{-}HNC)_2(OH)_4]^{2-}$ units (**10**) (C_{2v} with the *x* axis as C_2). An interaction diagram for the binuclear unit **10** is given in Figure 8. The interaction between the π_d orbital of $[Pd_2(OH)_4]^{2-}$ and the occupied σ orbital of HNC has a good overlap and leads therefore to an important stabilization of the bonding combination. This bonding interaction is presumably responsible for the linear structure of bridging isocyanides found in the crystal structure of **5a**. The π_d* orbital of $[Pd_2(OH)_4]^{2-}$ interacts with the empty π* orbital of HNC, which formally leads to a transfer of electrons from the Pd_2 unit to the isocyanides. However, the energy gain of this interaction is relatively small, and the observed linear structure of isocyanides implies that such interaction is eventually weak. On combining two $[Pd_2(\mu\text{-}HNC)_2(OH)_4]^{2-}$ units to a distance of 2.90 Å, no stabilizing energy is formed, and a slight destabilization is actually made (+0.30 eV) by repulsive interactions between the a_1 and b_1 orbitals (hybrid of d_{z^2} and $d_{x^2-y^2}$) of the two Pd_2 units, suggesting that the long Pd–Pd distance of ~2.9 Å is ascribable to the conformational advantage of $Pd_2(OAc)$ ring.

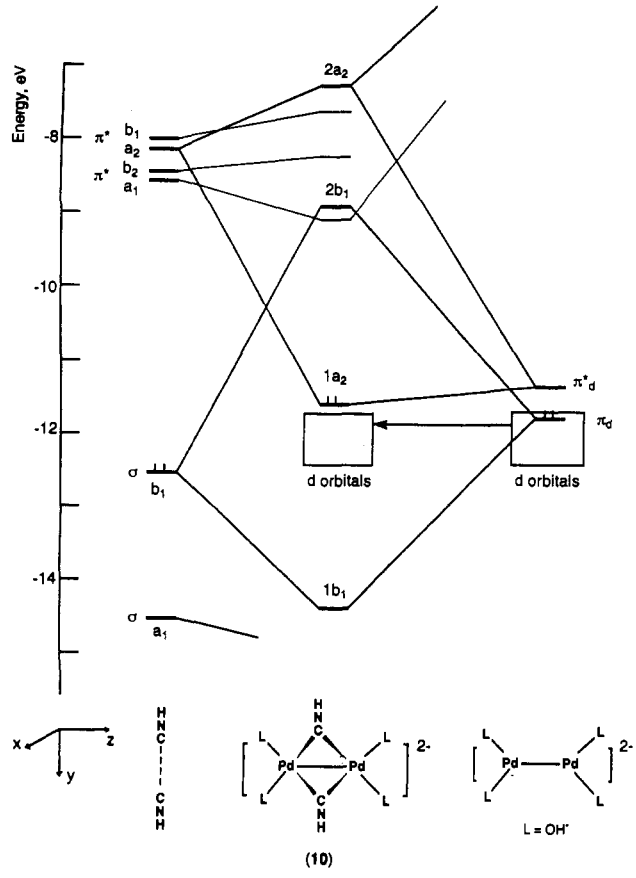

Figure 8. Interaction diagram for the valence orbitals of $[Pd_2(\mu\text{-}HNC)_2(OH)_4]^{2-}$ (**10**).

Supplementary Material Available: Figures 1 and 5, showing NMR spectra, and listings of crystallographic data, positional and anisotropic thermal parameters, atomic parameters of the hydrogen atoms, and bond distances and angles for **3a**, **3b**, and **5a** (24 pages). Ordering information is given on any current masthead page.

(37) Donohue, J. The Structure of Elements; Wiley: New York, 1974; p 216.
(38) Andrianov, V. G.; Biryukov, B. P.; Struchkov, J. T. *J. Struct. Chem.* **1969**, *10*, 1129.
(39) Churchill, M. R.; Mason, R. *Nature* **1964**, *32*, 194.
(40) Yamamoto, Y. *Coord. Chem. Rev.* **1980**, *32*, 194.
(41) Moiseev, I. I.; Stromrova, T. A.; Vargaftig, M. N.; Mazo, G. J. *J. Chem. Soc., Chem. Commun.* **1978**, 27.